Supporting information

Characterization of the synthesized catalytic materials

The morphology of the PdQDs@C-CeOx/RGO catalyst was characterized by high resolution transmission electron microscopy (HRTEM, JEM 2100, JEOL), field emission electron microscopy (FETEM, JEM 2200FS, JEOL), and energy dispersive X-ray spectroscopy (SEM, JEOL 6300, EDX, Oxford Instruments). The crystal structure of the catalytic material was characterized by powder X-ray diffraction (XRD, Bruker D8 discover). The Raman spectra were obtained using a Nanofinder 30 from Tokyo Instruments (laser source: 633 nm). The electrochemical properties of the catalysts were assessed on an electrochemical workstation (Biologic 320V) using a three-electrode system where the Pd@C-CeOx/RGO catalyst-modified glassy carbon, a platinum wire, and a saturated calomel electrode served as the working electrode, counter electrode, and reference electrode, respectively

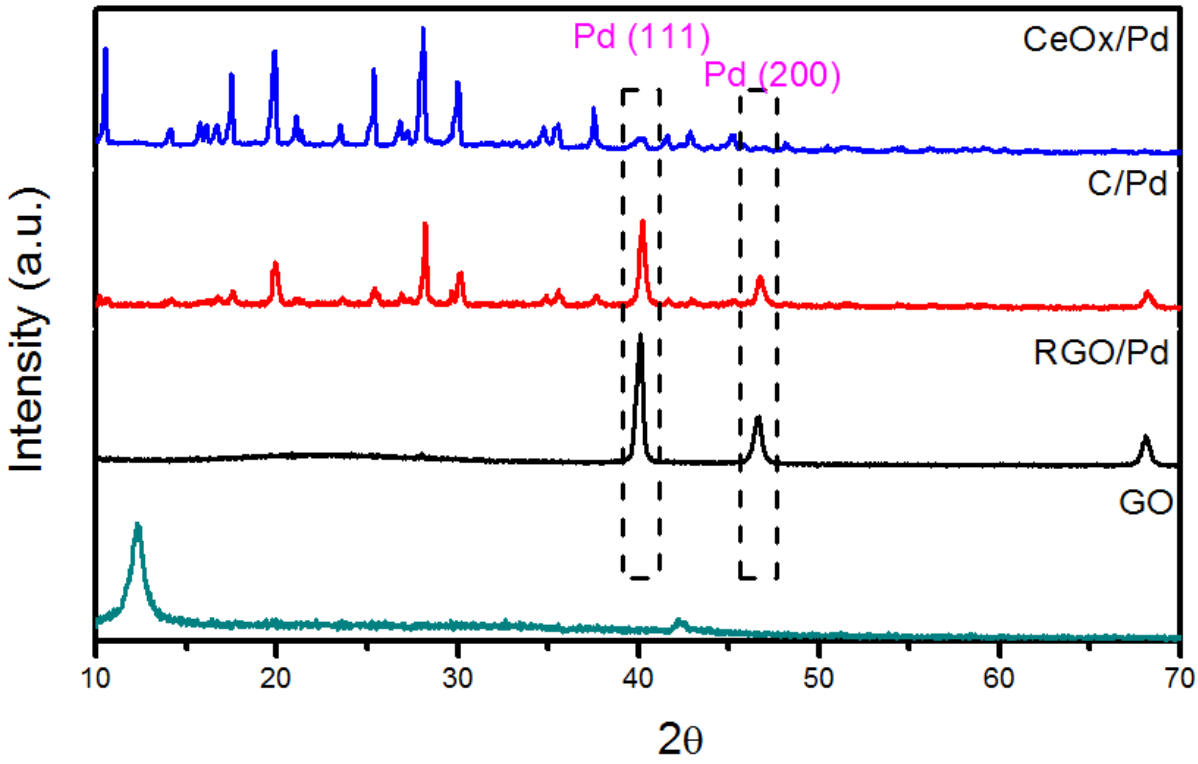

Fig. S1. XRD patterns for Pd nanoparticles on various supports

The XRD patterns of GO exhibits characteristic C(002) peak at 2q=10.3°, where after reaction with Pd and ascorbic acid, the C (002) peak disappeared and a new broad peak around 22 is appreared , which indicates during the reduction process the GO is converted in to RGO. The Pd nanoparticles exhibits peaks at 40.1 (Pd (111)) and 45.6 (Pd (200)). The similar XRD peaks for Pd is observed in CeOx and Carbon supports also.

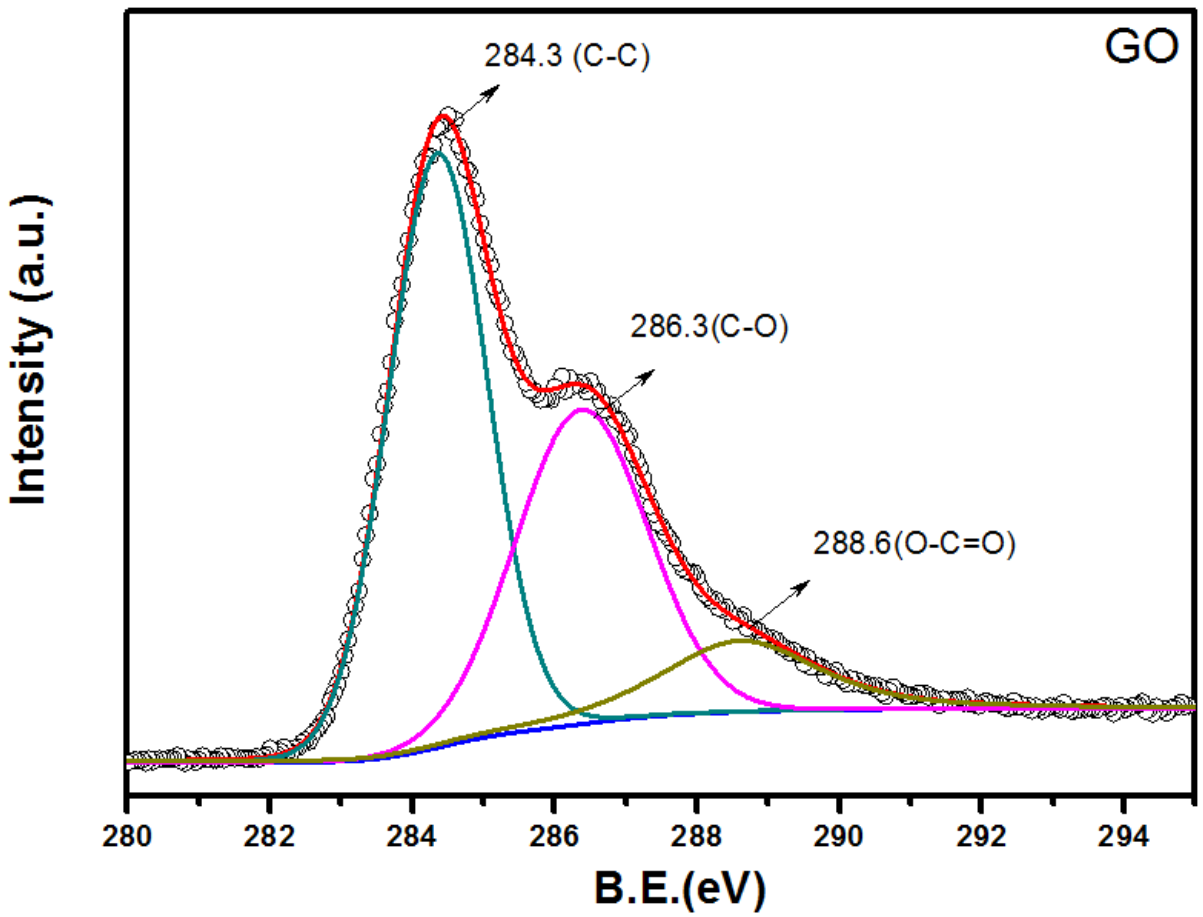
GO
284.3 (C-C)
286.3(C-O)
288.6(O-C=O)
Intensity (a.u.)
B.E.(eV)
280
282
284
286
288
290
292
294

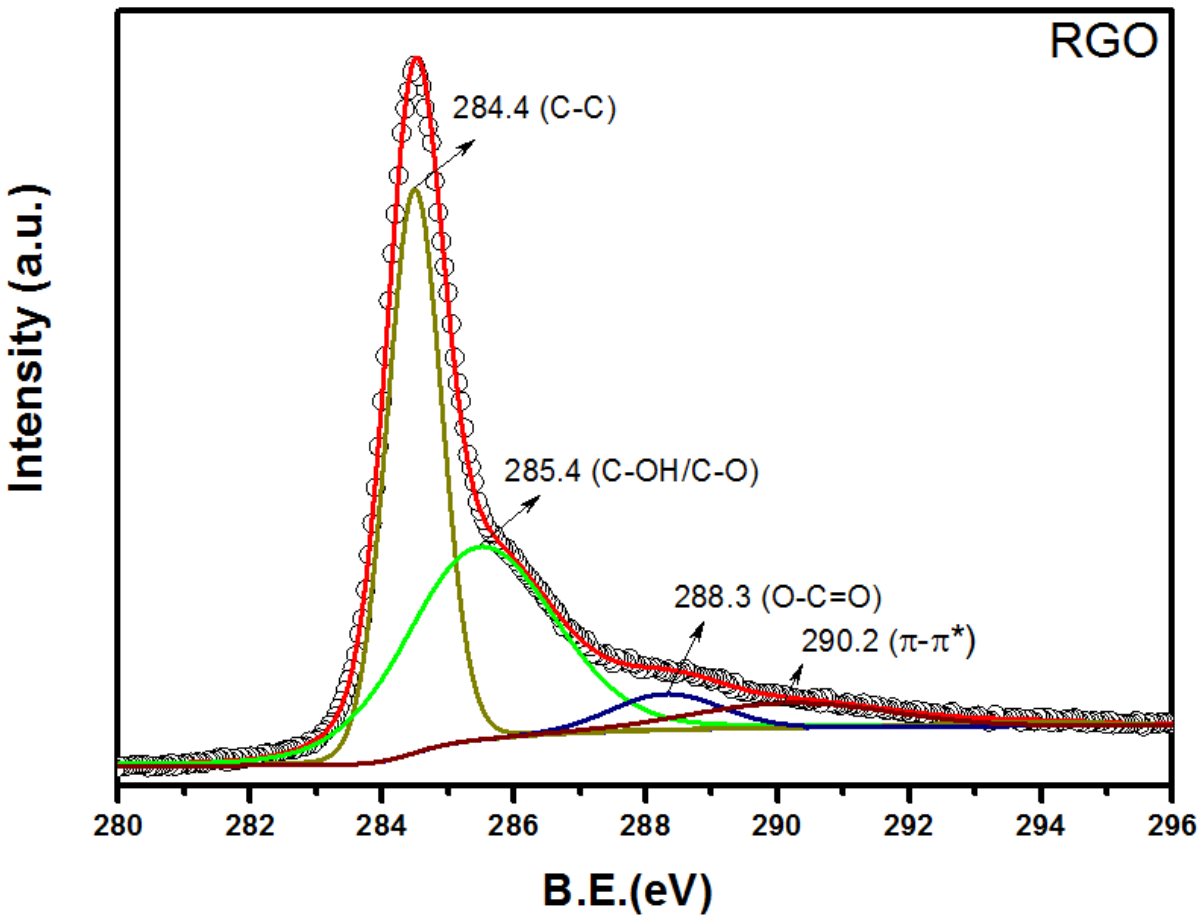
RGO
284.4 (C-C)
285.4 (C-OH/C-O)
288.3 (O-C=O)
290.2 (π-π*)
Intensity (a.u.)
280
282
284
286
288
290
292
294
296
B.E.(eV)

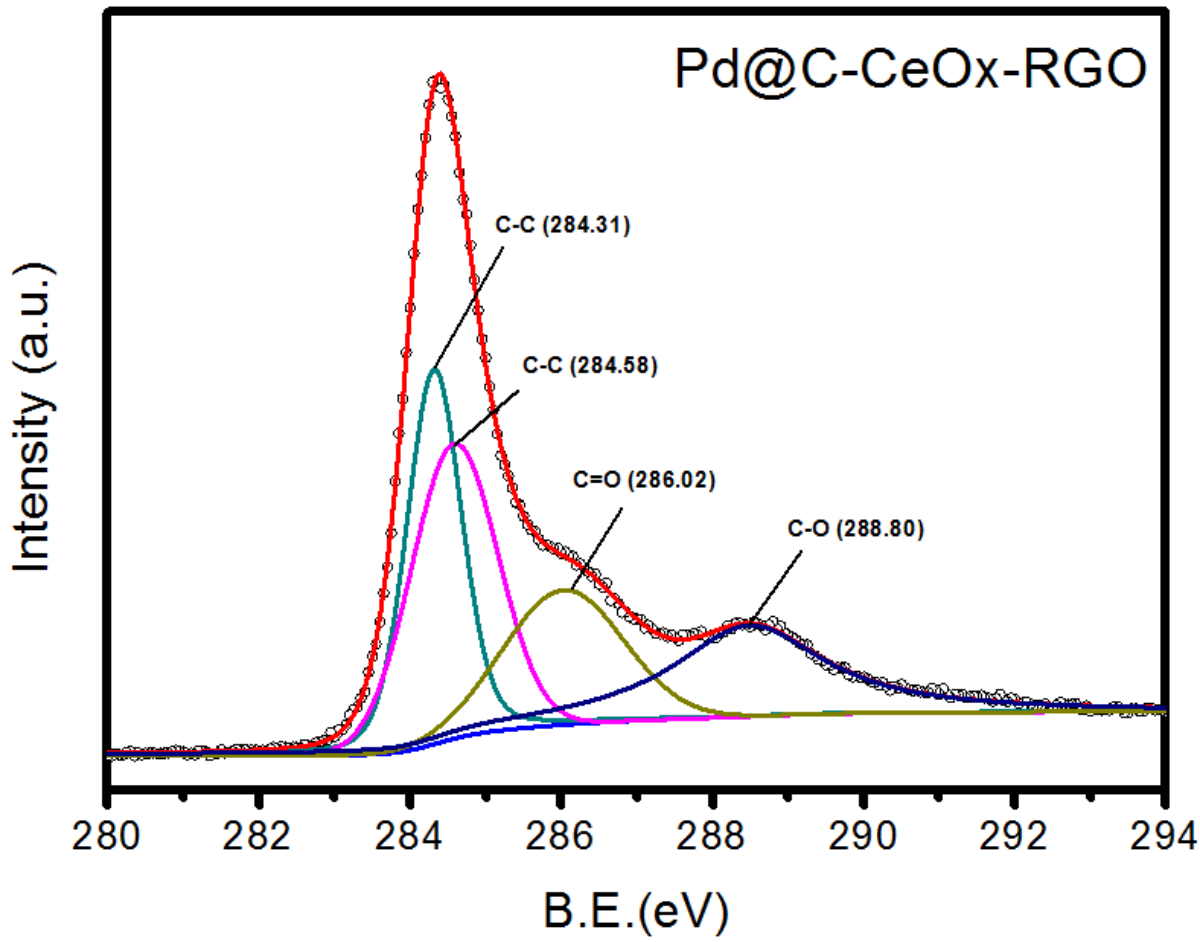

Fig. S2. Deconvoluted C1s XPS spectrum of GO, Pd-CeOx/RGO and PdQDs@C-CeOx/RGO (insitu carbon generated Pd@c-CEOx/RGO hybrid nanostructures)

The Deconvoluted C1s XPS spectrum of GO, Pd-CeOx/RGO and Pd QDs@C-CeOx/RGO are shown in Fig.S2. The C-O peak intensity is high in GO, whereas after reduction i.e, RGO , the C-O intensity is reduced significantly. After the formation of carbon particles, the C-C peak intensity and the C-O peak intensity increases, and shift in the peak position of C-C from 284.4 to 284.31 eV, attributes to the formation carbon in the catalyst.

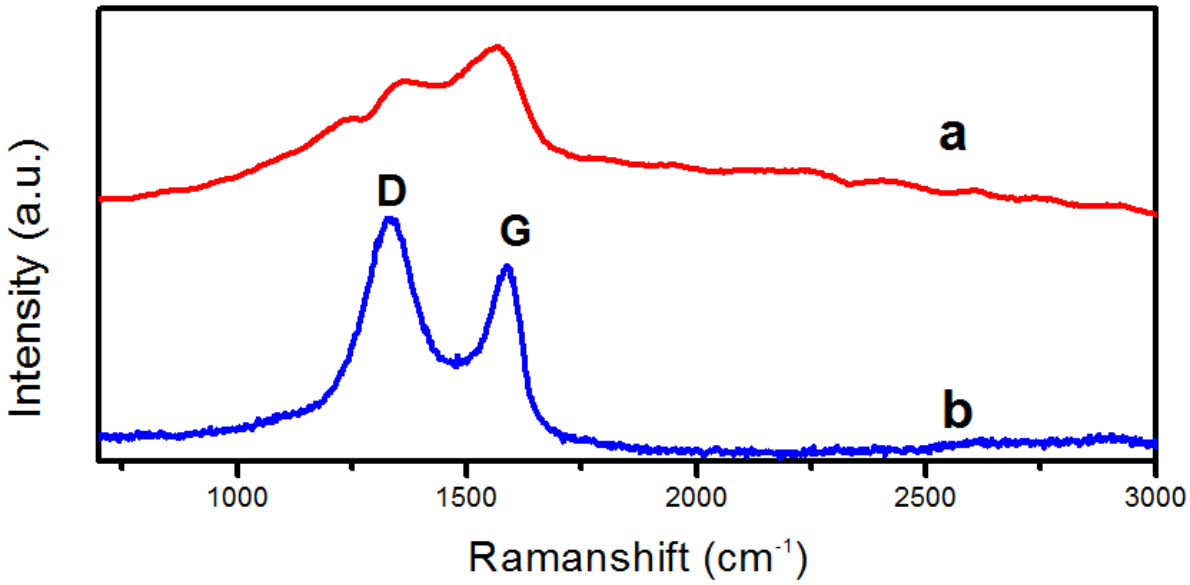

Fig.S3. Raman Spectra for (a) Pd QDs-CeOx/GNS and (b) Pd QDs@C-CeOx/GNS

The Raman spctra for Pd QDs over CeOx/GNS (a) before and (b) after microwave heat treatments, the results indicate the intensity of D and G ratio for the unheated sample shows higher D and lower G, whereas microwave subjected sample the $I_D > I_G$, the higher D band indicates the formation carbonous materials from reductant [*T. Wang, H. Wang, X. Chi, R. Li, J.Wang, Carbon 74 (2014) 312; R. Kannan, A. R. Kim, H.K. Lee, K.S. Nahm, D. J. Yoo, Chem.Commun. 50 (2014) 14623*].

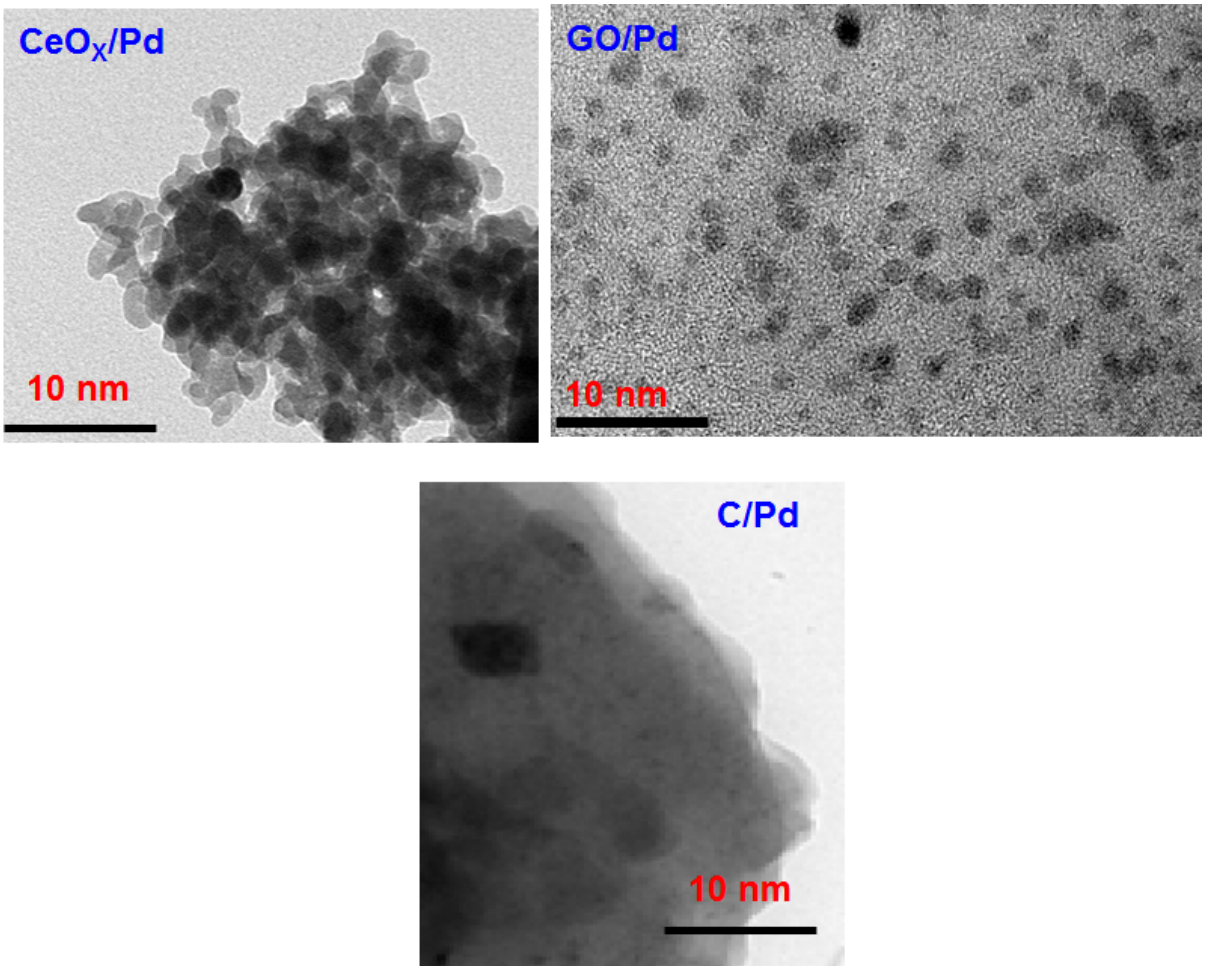

Fig. S4. TEM micrograph of Pd on various supports CeOx, GO and C.

,

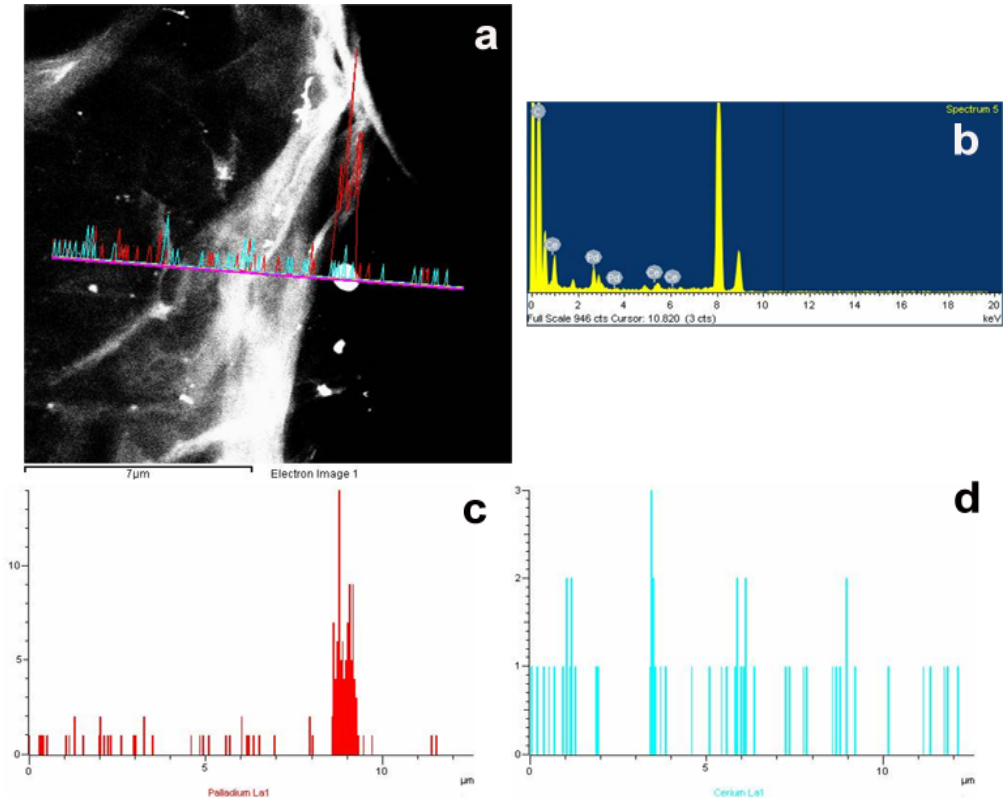

Fig.S5. (a) HAADF-STEM micrograph, (b) EDS, and (c) Pd and Ce distributions of Pd@C-CeOx/RGO hybrid nanostructures.

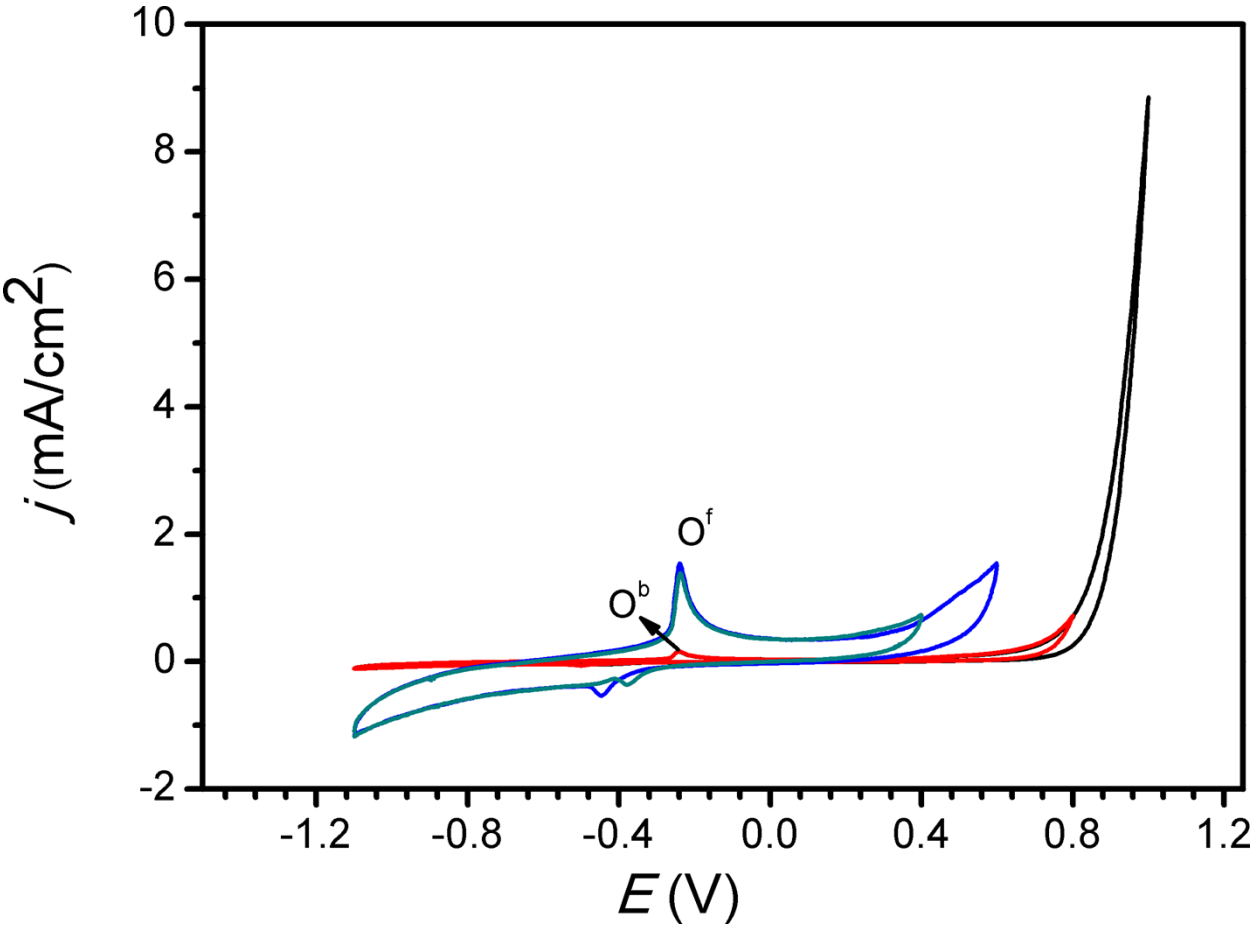

Fig. S6. CVs for the electrooxidation of methanol at Pd QDs dispersed GNS electrode at various $E_{upper.}$ (+0.2 to +1.0 V)

As the E_{upper} reached +0.4 V, the Pd oxidized and the corresponding reduction peak observed at -0.38 V, further increament to +0.6 V, the reduction current increased peak current and also shifted to the lower potential. Whereas, further increment in the Eupper, the O^f peak current is reduced significantly, indicates the electrocatalytic activity is reduced or suppressed. Which indicate the coverage of less active Pd in the catalyst [*L. D. Burke and J. K. Casey, J. Appl. Electrochem. 23 (1993) 573-582*].

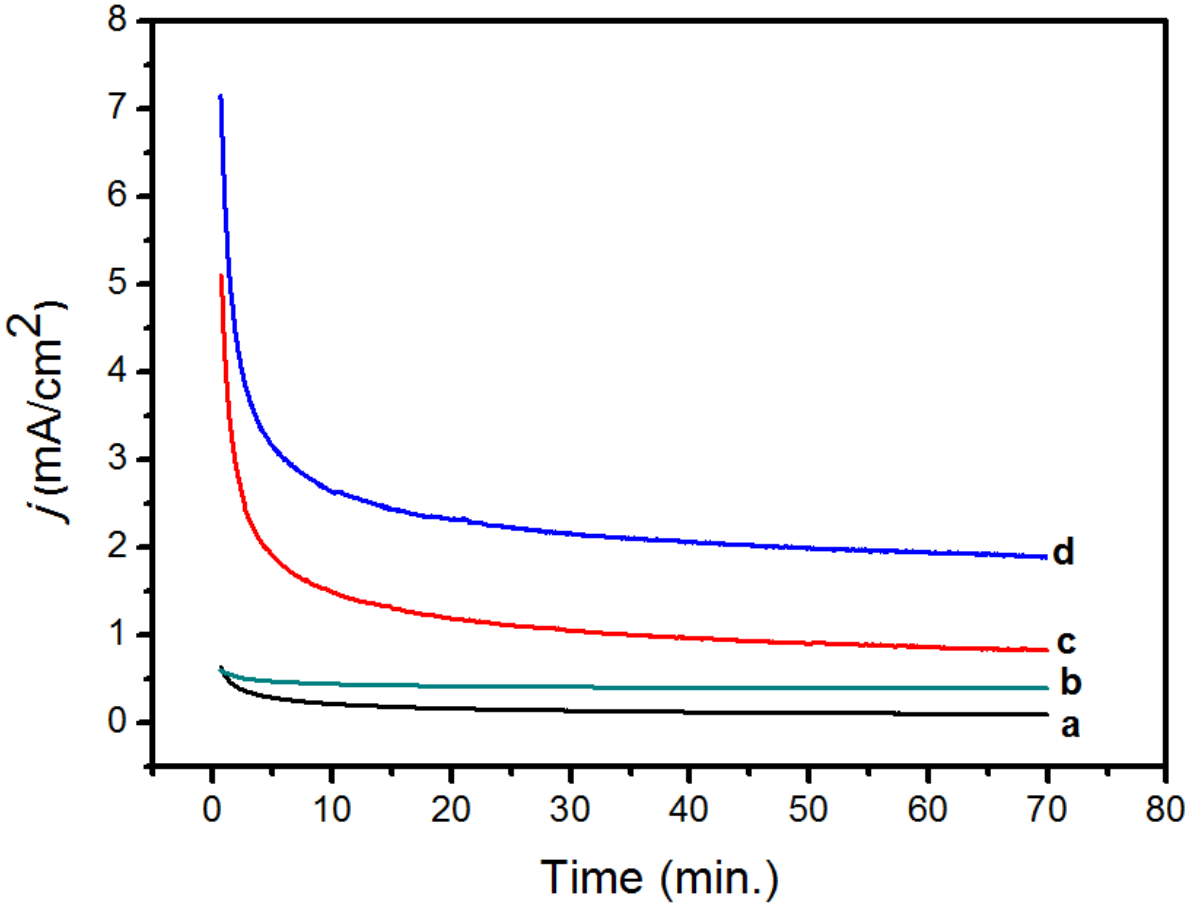

Fig.S7. Chronoamphermetric studies at (a) Pd/CeOx, (b) Pd/RGO, (c) Pd-CeOx/RGO, and (d Pd@C-CeOx/RGO electrodes in 1 M KOH / 0.5 M EG.